Published in final edited form as:
ACS Chem Biol. 2013 August 16; 8(8): 1764–1774. doi:10.1021/cb4000103.

In vitro and *in vivo* Characterization of a Tunable Dual-Reactivity Probe of the Nrf2-ARE Pathway

Rui Wang[†], **Daniel E. Mason**[‡], **Keith P. Choe**[||], **Alfred S. Lewin**[#], **Eric C. Peters**[‡], and **Hendrik Luesch**[*,†]

[†]Department of Medicinal Chemistry, University of Florida, Gainesville, Florida 32610, United States

[||]Department of Biology, University of Florida, Gainesville, Florida 32610, United States

[#]Department of Molecular Genetics and Microbiology, University of Florida, Gainesville, Florida 32610, United States

[‡]Genomics Institute of the Novartis Research Foundation, San Diego, California 92121, United States

Abstract

The cell utilizes the Keap1/Nrf2-ARE signaling pathway to detoxify harmful chemicals in order to protect itself from oxidative stress and to maintain its reducing environment. When exposed to oxidative stress and xenobiotic inducers, the redox sensitive Keap1 is covalently modified at specific cysteine residues. Consequently, the latent transcription factor Nrf2 is stabilized and translocates into the nucleus, where it transactivates the expression of detoxification genes through binding to the antioxidant response element (ARE). In the pursuit of potent and bioavailable activators of the ARE, we validated hits from a pathway-directed high-throughput screening campaign by testing them in cell culture and a reporter strain of a whole animal model, *Caenorhabditis elegans*. These studies allowed us to identify AI-3 as an ARE activator that induces cytoprotective genes in human cells and in worms, which also translated into *in vivo* activity in mice. AI-3 is an electrophilic ARE activator with two thiol sensitive sites towards a nucleophilic aromatic substitution, and SAR studies indicated the tunability of the system. Tandem LC-MS analysis revealed that AI-3 alkylates Keap1 primarily at Cys151, while AI-3 is reactive towards additional cysteine residues at higher doses *in vitro* and *in vivo*. The immediate effects of such alkylation included the disruption of Keap1-Cul3 (low [AI-3]) and/or Keap1-Nrf2 (high [AI-3]) interactions that both led to the stabilization of Nrf2. This further translated into the downstream Nrf2-ARE regulated cytoprotective gene activation. Collectively, AI-3 may become a valuable biological tool and may even provide therapeutic benefits in oxidative stress related diseases.

INTRODUCTION

The activation of the nuclear factor E2-related factor 2 (Nrf2)-antioxidant response element (ARE) mediated defense signaling pathway has been increasingly studied to tackle oxidative

[*]Corresponding Author: luesch@cop.ufl.edu.

Notes

The authors declare no competing financial interest.

Supporting information

Detailed SAR data, Supporting Figures, and experimental procedures are available free of charge via the Internet at http://pubs.acs.org.

stress related health problems, such as inflammation, cancer, and many age-related diseases[1–6]. The Nrf2 protein is an inducible cap 'n' collar type transcription factor that is responsible for activating the expression of a variety of antioxidant proteins and cytoprotective enzymes. Under normal conditions, its repressor Keap1 serves as an adaptor for Cul3-based E3 ubiquitin ligase complex to target Nrf2 for proteasomal degradation. However, when the cell is exposed to stressors, changes in Keap1 lead to the dissociation of the Cul3 complex, resulting in discontinuation of Nrf2 ubiquitination. This in turn promotes the accumulation of Nrf2, its nuclear translocation, and the subsequent binding to the ARE that regulates the expression of many cytoprotective proteins, such as NAD(P)H:quinone oxidoreductase 1 (NQO1) and glutathione *S*-transferase (GST)[7](Figure 1a).

There are six functional domains (Nrf2-ECH homology 1–6, or Neh1-6) in Nrf2. The C-terminal Neh1, Neh4 and Neh5 domains are important for ARE binding and transactivation, whereas the N-terminal Neh2 domain is responsible for binding with Keap1 through its DLG and ETGE motifs[8]. Keap1 possesses three functional domains, the N-terminal Broad complex, Tramtrack, and Bric-a-Brac (BTB) domain, the intervening region (IVR), and the C-terminal DC domain that encompasses the double glycine repeat or Kelch repeat (DGR) and the C-terminal region (CTR). In a healthy cell, the N-terminal BTB domains of two molecules of Keap1 form a homodimer with the two C-terminal 'arms' (the DC domains) that 'hold' each of the DLG (lower affinity) and ETGE (high affinity) motifs in the Neh2 domain of Nrf2. This specific positioning allows the Cul3-E3 ubiquitin ligase that also binds at the BTB region to ubiquitinate the seven lysine residues between the DLG and ETGE motifs[9].

Keap1 senses oxidative stressors through its cysteine residues, or the so-called 'cysteine codes'[10]. Distinct cysteine residue(s) are recognized by specific sets of chemicals to each elicit their unique patterns of downstream molecular effects. Out of the twenty-seven cysteines on Keap1, three (Cys151, Cys273, and Cys288) were conceded to be the sole or collaborative player(s) in Keap1-Nrf2 signaling in various cell types[11]. Cys151 is located in the BTB domain. Modifications at this particular site have been shown to result in the dissociation of the Cul3-ubiquitin ligase complex[12], possibly perturbed by the molecular volume increases at Cys151[13], which also agrees with the earlier findings that mutations of the cysteine to a less electrophile sensitive serine renders the Keap1-C151S an inactive oxidative stress sensor[14]. In contrast, manipulations of the two IVR cysteines Cys273 and Cys288 were found to retain Keap1-Cul3 interaction[15], but instead lead to the dissociation of the low affinity Nrf2 DLG domain from Keap1[16] so that it may no longer be able to hold Nrf2 in the correct conformation for ubiquitination[17], in accordance with the constitutive activities of Nrf2 found in the presence of Keap1-C273S or Keap1-C288S[14].

We have previously identified multiple electrophilic activators of the ARE from a synthetic library of 1.2 million small molecules using an ARE-luciferase reporter assay in high-throughput screening (HTS) format. One particular compound, AI-1 (ARE Inducer-1), was already investigated in detail as an *in vitro* probe due to its bioactivity in primary cortical culture and low toxicity, which also led to the more active AI-2[18]. The aims of the present study were to examine the suitability of any of these compounds as *in vivo* probes and to subsequently elucidate the chemical and biological mechanisms of action of the prioritized activator(s), with the ultimate goal of enriching the tool box to study this disease-relevant pathway.

RESULTS AND DISCUSSION

We established a comprehensive *in vitro* and *in vivo* assay platform to filter hits and utilized chemical sub-libraries to interrogate the link between structural changes and specific

functional consequences on the molecular level. This combination of organic chemistry, biochemistry, molecular biology and proteomics allowed us to study the system at high resolution and discover new ways to manipulate the Keap1/Nrf2-ARE pathway.

Identification of a potent ARE activator, AI-3

Of the seven originally prioritized HTS hits, six were commercially available (Figure 1b) and validated by using the same ARE-luciferase (ARE-luc) reporter assay in a dose-response manner in IMR-32 cells[18] (Figure 1c). While, as expected, AI-1 was not toxic up to 32 μM, the other molecules showed signs of cytotoxicity beyond 10 μM. However, at 10 μM the ARE-luc activity of AI-1 (31.4-fold) was at least 40% lower than most of the others (52.2- to 96.1-fold).

To ensure that these activities from the ectopic reporter system translated into endogenous gene activation and that they were not due to oxidative stress, the small molecules were tested by Western blot analysis for their ability to induce the ARE-driven gene NQO1 in the presence of a cell permeable antioxidant (*N*-acetylcysteine, NAC)[18,19](Figure 1d). The endogenous gene activation results were consistent with the ARE-luc data. All compounds induced NQO1 in a dose-dependent manner. At the maximum non-toxic concentration (10 μM), the levels of NQO1 were similar both in the presence and the absence of the NAC, suggesting that the groups of small molecules did not activate the ARE by exerting oxidative stress to the cell.

We then examined the abilities of these small molecules to induce cytoprotective genes in a whole-animal model predictive of bioavailability, the transparent free living nematode *Caenorhabditis elegans*. The relatively small size (~1 mm) and short life span (2–3 weeks) allow the worms to be cultured in microtiter plates and widely used as biosensors in agricultural[20] and pharmaceutical industries[21,22]. Similar to vertebrates, they have a thiol-sensitive cytoprotective pathway (Figure 1a) that is also inducible[23]. The detoxification of oxidative insults is controlled through a cytoplasmic transcription factor, SKN-1, a homologue of Nrf2. Under basal conditions, SKN-1 constantly translocates into the nucleus and is targeted for Cul4-dependent proteasomal degradation by the repressor, WDR-23, a functional equivalent of Keap1[24,25]. When the cell experiences oxidative stress, SKN-1 bypasses WDR-23 and activates the expression of cytoprotective genes, such as glutathione *S*-transferase 4 (*gst-4*)[23].

By utilizing a reporter strain of *C. elegans*, the *in vivo* bioactivities of the compounds were assessed in a dose-response manner (Figure 1e). Compound **6** stood out to be a remarkably potent *gst-4* activator (22.5-fold) in *C. elegans* up to 1 mM (the highest non-toxic concentration), while dose-dependent activation was also detected for other compounds (**1**, **3**, and AI-1), but to a much lesser extent (2.4- to 5.6-fold). Compound **6** was given the name AI-3 (ARE Inducer-3) since it originated from the same screen as AI-1. The promising *in vivo* data in *C. elegans* motivated us to test AI-3 in a higher organism.

In vitro stability and *in vivo* bioactivity of AI-3 in mice

Metabolic stability is a desired property in discovering potential drug leads[26]. Before subjecting AI-3 to a rodent model, we assessed its *in vitro* stability in mouse plasma over a period of 24 h (Figure 2a). AI-3 showed remarkable plasma stability (78%) up until 24 h, suggesting great potential of extended bioavailability. When incubated with human embryonic kidney cell lysate (HEK293), the levels of AI-3 gradually decreased in a time-dependent manner ($t_{1/2}$ ~12 h), indicating that AI-3 can be slowly metabolized by cellular components (Figure 2a). In mouse liver microsomes supplemented with NADPH (Figure 2b), AI-3 was more quickly metabolized (~8% remaining after 2 h) yet considered of

medium to high metabolic stability ($t_{1/2}$ ~20 min) based on a scoring system proposed by Di *et al*.[27].

AI-3 was then administered to 4-week-old mice via intraperitoneal single-dose injection (50 mg/kg). Upon 12 h treatment, the mRNA levels of the ARE-regulated gene *Nqo1* were assessed in liver and kidney tissues by quantitative PCR (qPCR) after reverse-transcription (RT) (Figure 2d). Elevated *Nqo1* transcript levels were detected in both organs with statistically significant induction in the liver (5.5-fold). Additionally, we found that multiple other Nrf2-regulated genes[28] were induced by AI-3 in the liver tissues (Figure 2e).

These initial validation results led us to prioritize AI-3 as it showed bioactivity in mammalian cell cultures with *in vivo* activity in *C. elegans* and in mice. Therefore, we decided to investigate the chemical and biological modes of action of AI-3.

Chemistry

A common structural feature shared by many ARE activators is the electrophilic Michael acceptor motif. This chemical signal can be recognized by the nucleophilic sulfhydryl groups, i.e., cysteine residues on Keap1, to trigger the activation of downstream pathways[29]. AI-3 is comprised of two potential Michael acceptor systems. First, it has a unique, enone motif in that it is an acylated electron-deficient heteroaromatic (thiophene) system substituted in β-position to the carbonyl group with a methyl sulfonyl group that could act as a leaving group in a nucleophilic aromatic substitution (addition-elimination) reaction. Second, the conjugated methyl sulfonyl group can also act as an acceptor of π-electrons in a Michael-type fashion[30] (Figure 3a) and in corresponding δ-position there is a second electrophilic, chloro-substituted carbon (C1) position where an addition-elimination (nucleophilic aromatic substitution) reaction can occur. We speculated that both substituents may contribute to the reactivity of AI-3 towards sulfhydryl groups through addition-elimination reactions at two sites.

To test this hypothesis, an *in vitro* alkylation experiment was conducted in which AI-3 was incubated with excess of each of two biologically relevant small molecule thiols (NAC and glutathione (GSH)) for 2 h at room temperature (r.t.) (Figure 3b). The reaction products were then analyzed by LC-MS. Substitution products at the methyl sulfonyl- and chlorine-position were detected for both nucleophiles.

Having identified the sulfhydryl sensitive sites on AI-3, we next examined how alterations of the chemical scaffold and electronics of the aromatic ring would affect its bioactivity. Using the ARE-luc reporter assay, we tested thirty-two synthetic analogs of AI-3 in a dose-response manner (Table S1). We found that monosubstitutions at either thiol-reactive position led to changes in bioactivity profiles. First, a methyl sulfonyl group or related π-electron acceptor proved to be critical for AI-3's ARE activity. When it is replaced with a methyl sulfide group (AI-3-1, **7**), which can act neither as an electron-acceptor nor a good leaving group, both potency and efficacy were reduced. AI-3-1 (EC_{50}, 11.2 μM) was 2.5 times less potent than AI-3 (EC_{50}, 4.4 μM), and its maximum efficacy dropped to 19% (5.7-fold at 32 μM) as compared with the parent compound (30.4-fold at 10 μM). Substitution with a methyl sulfoxide group (AI-3-2, **8**) that is not as good a leaving group as the methyl sulfonyl group yet can act as π-electron acceptor enhanced the biological profile by shifting the EC_{50} from 4.4 μM (AI-3) to 1.0 μM (AI-3-2 was toxic at 10 μM), while sustaining the maximum potency (31.1-fold at 3.2 μM vs. 30.4-fold). Secondly, manipulations at the chloro-position showed that this functional group is important but not the primary determinant of bioactivity. The corresponding unsubstituted analog (AI-3-3, **9**) retained 63% of the efficacy (19.2-fold vs. 30.4-fold, both at 10 μM) while the potency increased by 1.5 times (EC_{50}: 2.9 μM vs. 4.4 μM). The analog bearing the less electronegative bromine

substituent (AI-3-4, **10**) had roughly the same ARE-luc activity at 10 μM while its potency increased by 1.7 times (EC_{50}: 2.6 μM vs. 4.4 μM), indicating that the better leaving group potential was able to offset electronic effects on the ring that would otherwise decrease reactivity. These results indicated that the role of the chlorine may be either to affect the electronics of the thiophene ring and therefore the electrophilicity of the second reactive carbon C3, or to serve as a leaving group to facilitate the nucleophilic attack at C1, suggesting the tunability of the system by modulating these two parameters.

Regardless of the leaving group potential of the C1 substituents, the analogs rendered inactive as long as the methyl sulfide group or equivalent was in C3 position (**13–16**, **20–25**, **27**, **32**), indicating that π-electron withdrawing substituents (through conjugation) are needed at C3 in order to activate C1's reactivity towards (thiol) nucleophiles. With a methyl sulfoxide group at C3, the maximum efficacy is modulated depending on the nature of the electron-withdrawing group (EWG) at the C1 position (**17–19**). The carbonyl group at C4 is essential for bioactivity. Alterations at this site were not tolerated (**29**). The observed correlations between the functional groups and the bioactivity confirmed that AI-3 requires an EWG at the β-position (C3) of the Michael system for its bioactivity. The EWG can act either as a leaving group to undergo a formal Michael type addition-elimination reaction at C3 (nucleophilic aromatic substitution), or as an auxiliary group to facilitate a nucleophilic attack at C1 by increasing its electrophilicity. Other factors, such as the spatial requirements of the compound and noncovalent interactions with the local environment of the target may also play a role in the overall bioactivity.

AI-3 induces cytoprotective genes in IMR-32 cells

The ability of AI-3 to induce the ARE-regulated cytoprotective gene, *NQO1*, was tested both at the transcript and protein levels (Figures 4a, b), which appeared to be dose-dependent. At 12 h of treatment, *NQO1* mRNA levels increased starting from 0.03 μM (1.8-fold) and reached a plateau at 10 μM (27.7-fold). Based on immunoblot analysis, after 24 h of treatment, NQO1 protein levels started to heighten at 0.3 μM and also plateaued at 10 μM. Furthermore, as shown in Figure 1d, at lower concentrations (0.3 μM–3.2 μM), AI-3's NQO1-inducing activity was slightly reduced in the presence of NAC, an antioxidant that could also act as a thiol nucleophile (Figure 3b), thereby leading to somewhat reduced bioavailability of AI-3. Nonspecific reactivity with thiols would also suggest that there is potential for off-target toxicity, causing oxidative stress in the cell, which may be balanced out by NAC at lower concentrations, as observed for the oxidative stressor diethyl maleate (DEM) (Figure 1d)[31]. To rule out the latter possibility, two sets of experiments were performed. First, cellular levels of reactive oxygen species (ROS) were measured after the cells were treated with serial dilutions of AI-3; ROS levels in the cell remained largely unaffected (Supporting Information, Figure S1). Secondly, the levels of NQO1 were tested in the presence of a second antioxidant, catalase[32,33] (Figure 4b). AI-3 induced NQO1 to similar levels at all concentrations tested, indicating that the previous observation may be due to the thiol-reactive nature of the compound. In addition, AI-3 was also found to induce multiple other Nrf2-regulated genes in IMR-32 cells (Figure 4c).

The most abundant free thiol in the cell is the small molecule antioxidant glutathione[34]. With *in vitro* evidence that AI-3 may be GSH reactive (Figure 3b), the influence of AI-3 on intracellular levels of GSH was examined in IMR-32 cells (Figure 4d). The endogenous glutathione levels were indeed reduced by 30% after 2 h, consistent with the observed direct sulfhydryl reactivity of AI-3 *in vitro* (Figure 3b). This may potentially also be due indirectly to AI-3 related temporary disruption of cellular redox state that would have consumed GSH to restore. Yet, the loss of GSH was compensated for by 8 h and the levels continued to increase until 24 h (160%). One potential explanation is that the temporary partial depletion

of GSH directly by AI-3 may induce a feedback signal to activate the Nrf2-ARE system that controls the GSH biosynthetic and recycling genes[28] (Figure 4c).

AI-3 requires Nrf2 and PI3K for its bioactivities in IMR-32 cells

While certain small molecules induce both *Nrf2* mRNA production through the activation of the upstream aryl hydrocarbon receptor (AhR)-xenobiotic response element (XRE) signaling pathway and Nrf2-regulated gene activation[35], others are mono-functional inducers that only modulate phase II enzyme expression. Figure 4a showed that treatment with AI-3 did not have any effect on *NRF2* mRNA levels, suggesting that it is a specific inducer of the phase II response. To confirm the involvement of Nrf2 in the activation of cytoprotective genes, we employed small interfering RNAs (siRNA) to knock down endogenous *NRF2* transcripts for 48 h. The cells were then treated with AI-3 for 24 h (Figure 5a). The expression of NQO1 was significantly reduced corresponding to the knock-down efficiency of si*NRF2* used (~75%, Supporting Information, Figure S2)[19,36], indicating that Nrf2 is essential in AI-3-induced *NQO1* gene induction. We next examined the effect of AI-3 on the stabilization and nuclear translocation of Nrf2[32] over a period of 18 h (Figure 5b). After 1 h, Nrf2 was detectable in the nucleus, and its level remained increased to the same extent after 3 h. Moreover, the Nrf2-ARE regulated expression of NQO1 was observed starting from 12 h and continued to increase until 18 h, further testifying that Nrf2 nuclear translocation precedes and is needed for ARE-regulated gene activation and expression.

In addition to Keap1 alkylation-initiated Nrf2 activation, phosphorylation of Nrf2 through kinase signaling cascades has been reported to affect Nrf2 activity. Functional phosphoinositide 3-kinase (PI3K) was required for AI-1/tBHQ-induced ARE activation in IMR-32 cells[18,37], whereas mitogen activated protein kinase (MAPK) signaling pathway was found to be essential for tBHQ's ARE activity in HepG2 cells[38]. To identify which one is needed for AI-3's ARE activity in IMR-32 cells, specific pharmacological inhibitors of both kinases were used to co-treat the cells with AI-3 (Figure 5c). AI-3 did not induce the expression of NQO1 in the presence of PI3K inhibitor (LY294002), whereas NQO1 levels were unaffected when co-treated with MAPK (MEK1) inhibitor (PD98059). This result indicated that PI3K kinase signaling is crucial for the activation of ARE-regulated genes by AI-3 in IMR-32 cells.

To further investigate the involvement of PI3K, nuclear levels of Nrf2 were examined after the cells were co-treated with AI-3 and the PI3K inhibitor (LY294002) (Figure 5d). Co-treatment with LY294002 reduced the levels of Nrf2 in the nucleus, which may be attributed at least in part to decreased Nrf2 translation due to PI3K inhibition[18]. However, even residual Nrf2 protein in the nucleus appeared to be transcriptionally inactive as evidenced by the lack of NQO1 expression (Figure 5c), suggesting that PI3K-mediated phosphorylation of Nrf2 is still necessary. Studies have shown that GSK-3 may be involved in small-molecule mediated Nrf2 activation through PI3K/Akt signaling pathway[39,40]. The phosphorylation status of Akt (downstream of PI3K) and GSK-3 (downstream of Akt) was measured to examine the involvement of GSK-3α/β over a period of 18 h (Figure 5e). No change in levels of phosphorylated GSK-3α/β observed at any of the times examined, which was consistent with similar levels of phosphorylated Akt in the presence or absence of AI-3. These results suggested that AI-3 does not modulate GSK-3α/β in the PI3K signaling pathway.

AI-3 recruits different sets of cysteine codes to dictate its biological activities

At the molecular level, the reactive cysteine residues on Keap1 seem to be recognized by chemical inducers with distinct structural features. While long-chain fatty acid type Michael acceptors (e.g., 15d-PGJ_2[10] and 9-nitro-octadec-9-enoic acid[15]) were found to have a

preference for Cys273 and/or Cys288, enone-compounds without a long fatty chain (e.g., tBHQ[10] and AI-1[18]) tend to favor Cys151. To test if AI-3's biological activities were also Cys151-dependent, we examined its effect on interactions between Keap1 and its molecular partners in the antioxidant defense system.

First, we investigated AI-3's influence on the functionality of Keap1 as an adaptor for the Cul3-ubiquitin ligase complex. Mammalian expression vectors encoding human Cul3 (hemagglutinin(HA)-tagged, HA-Cul3) and either wild type human Keap1 (chitin binding domain (CBD)-tagged, or wild type-Keap1) or Keap1-C151S (Cys151 mutated to Ser151, also CBD-tagged)[41] were co-transfected into HEK293 cells, which had been demonstrated to be suitable for overexpression experiments[18] and have low levels of endogenous Keap1 (Figures 6a–c). The cells were treated with serial dilutions of AI-3 for 5 h and Keap1 proteins subsequently purified by pull-down with chitin magnetic beads (Figure 6a). The amounts of wild type-Keap1-associated Cul3 were significantly reduced in the presence of AI-3; whereas the compound was unable to influence the levels of Cul3 associated with Keap1-C151S. This data suggested that AI-3's mechanism of action may involve Cys151.

Additionally, the association of Keap1 with Nrf2 in the presence of AI-3 was assessed. Plasmids carrying human Nrf2 (HA-tagged, HA-Nrf2)[41] and either wild type-Keap1 or Keap1-C151S were co-transfected into HEK293 cells that were then treated with increasing doses of AI-3 for 5 h before Keap1 protein was purified (Figure 6b). Treatment of cells overexpressing wild type-Keap1 with AI-3 did not disrupt Nrf2-Keap1 interactions, but led to the stabilization of Nrf2 starting from 3.2 μM. In the mutant (Keap1-C151S) transfected cells, no significant levels of Nrf2 were found to associate with Keap1 at lower concentrations (3.2 μM and 10 μM), consistent with the previous observation that Keap1-C151S was a constitutive repressor of Nrf2[14]. Perhaps surprisingly, we noticed that at higher concentrations (32 μM and 100 μM), treatment of AI-3 seemed to be able to reverse the repressive effect of Keap1-C151S and stabilize Nrf2, which was in contrast to the previous results that Keap1-Cul3 interactions were still intact at these concentrations (Figure 6a).

To further demonstrate that the AI-3-induced stabilization of Nrf2 was due to the dissociation of Cul3 from Keap1, i.e., due to the inhibition of Keap1-mediated ubiquitination of Nrf2, HEK293 cells were co-transfected with Neh2 (Gal4-tagged Keap1 binding domain on Nrf2, Gal4-Neh2), ubiquitin (HA-tagged, HA-Ub)[41] and either wild type-Keap1 or Keap1-C151S expression vectors. The cells were treated with the same concentrations of AI-3 for 5 h and Neh2 proteins then purified by immunoprecipitation (Figure 6c). The results corresponded to the last observation. Starting from 3.2 μM, AI-3 inhibited ubiquitination of Neh2 in the presence of wild type-Keap1. Again, Keap1-C151S was resistant to the inhibition at lower concentrations of the compound (3.2 μM and 10 μM), whereas it 'surrendered' at higher concentrations (32 μM and 100 μM) when lesser degrees of Neh2 ubiquitination were observed. This result raised our suspicion that AI-3 may employ more than one cysteine residue (Cys151) for its biological outcome in a dose-dependent manner. Therefore, we performed similar experiments by using a second Keap1 mutant (Keap1-C288S-CBD) to test the dependency of AI-3's effect on Cys288, another cysteine that is commonly involved in the Keap1-Nrf2 signaling. Our results showed that AI-3 induced dissociation of Cul3 from Keap1-C288S, which was probably due to alkylation at the Cys151 site (Figure 6d). Similar to previous reports that Keap1-C288S is a constitutive activator of the Nrf2[14], we found that Keap1-C288S stabilized Nrf2 (Figure 6e) and was not able to initiate Neh2 ubiquitination (Figure 6f).

To verify our results, we adapted an unbiased proteomics approach in which full-length human Keap1 protein was incubated with various concentrations of AI-3 for 30 min (Figure 7). LC-MS/MS analysis of the chymotryptic peptides indicated that the dominant modified

species was the peptide covering Cys151 (amino acid 1423154) with a mass increase of 212, resulting from a substitution reaction at C3 of AI-3 (Figure 7a). At higher concentrations and upon longer incubation times, additional Cys sites on Keap1 were modified by 212 adduction, especially Cys196 and Cys288 (Figures 7b, c). To assess the specific reactivity of AI-3 in a cellular context, we also analyzed Keap1 chitin pull downs from HEK293 cells overexpressing Keap1-CBD treated with 10 or 100 μM of AI-3. The same trend was observed in this *in vivo* setting (Figures 7d, e): dominant reaction of Cys151 at low concentration (10 μM) and additional reaction with mainly Cys196 and Cys288 at high concentration (100 μM). *In vitro* and *in vivo*, the 256 adduct resulting from substitution at C1 of AI-3 by cysteine residue was not detected under the same conditions.

The revelation that AI-3 recognizes the additional 'cysteine code' (Cys288) at high concentrations helped us understand the mechanisms underlying the conflicting results from the initial biological assessments for Keap1-C151S (Figures 6a–c). At lower concentrations, AI-3 was unable to stabilize Nrf2 because the compound was unable to alkylate the serine residue at the critical 151 position so that Cul3 was still associated with Keap1 and consistently targeted Nrf2 for proteasomal degradation. At higher concentrations, AI-3 caused Nrf2 stabilization through a distinct Cys151-independent mechanism by recruiting Cys288 in the IVR region in Keap1. As mentioned earlier, alkylation of this particular cysteine may lead to the release of the low affinity Nrf2/DLG motif from one 'arm' of Keap1[16]. Thus, Nrf2 may not be correctly positioned for ubiquitination even though the interaction between Cul3 and Keap1-C151S was still intact.

Conclusions

The work presented here detailed the complex chemical and biological mechanisms of actions of AI-3, a potent inducer of the Nrf2-ARE antioxidant defense system in two cultured cell lines and in two whole-animal models, and may have potential benefits as a therapeutic agent or tool compound. AI-3 is chemically tunable at two electrophilic carbons on the thiophene ring to direct the extent of true nucleophilic aromatic substitutions, unlike the nucleophilic pseudo-aromatic substitution reaction observed for AI-1[18]. In addition, AI-3 was also able to overrule the repressor function of a Keap1-mutant in a concentration-dependent manner, which may even give rise to new opportunities in chemically reversing mutation-induced functional consequences by targeting the cysteome with small molecules.

METHODS

Pgst4::GFP reporter gene assay in *C. elegans*

A strain of *C. elegans* (VP596, dvIs19[pAF15(*gst-4::GFP::NLS*)];vsIs33[*dop-3::RFP*]) carrying the reporter transgenes *Pgst-4*::GFP and *Pdop-3*::RFP was used[42]. The worms were treated with a solvent control (DMSO, 1–2%, v/v) or individual compounds for 24 h. The level of *Pgst-4* induction by each treatment was measured in a microplate reader and calculated as GFP /RFP.

Metabolic stability studies

AI-3 was incubated with mouse plasma, cell lysates, or microsomes for the indicated period of time. The reaction was then quenched and extracted with EtOAc, dried immediately under N_2 gas, reconstituted, and analyzed by HPLC-MS in positive mode with multiple reaction monitoring (MRM) scan.

In vivo alkylation of Keap1

Tagged Keap1-CBD plasmids were transfected into HEK293 cells which were then treated with AI-3 for 5 h. The AI-3-labeled Keap1-CBD protein was then pulled down by chitin

magnetic beads and further purified by SDS-PAGE. Keap1 protein was identified by Bio-Safe Coomassie Stain (Bio-Rad) stain and the gel bands were digested with chymotrypsin and analyzed by tandem LC-MS.

Detailed procedures of the above mentioned assays and all the other experimental procedures are described in the Supporting Information, including ARE-luc reporter gene assay, immunoblot analysis, mouse experiments, quantitative PCR, RNA interference assay, ROS detection, glutathione assay, chitin pull down, *in vitro* ubiquitination assay, HPLC-MS, and tandem LC-MS parameters.

Supplementary Material

Refer to Web version on PubMed Central for supplementary material.

Acknowledgments

This research was supported by the National Institutes of Health, grants R21CA133681, R21NS067678, and R01EY020825. The authors would like to thank H. Mao for performing i.p. injections and tissue harvesting from mice. We thank L. Rowland-Faux and L. Salvador for their assistance with LC-MS. We appreciate J. Johnson for sharing ARE-luc reporter; N. Gray and D. Zhang for sharing HA-Cul3, HA-Nrf2, HA-Ub, Gal4-Neh2, Keap1-CBD, Keap1-C288S-CBD and Keap1-C151S-CBD plasmids; and R. Tsien for sharing pcDNA3-mRFP through Addgene.

References

1. Kwak MK, Kensler TW. Targeting NRF2 signaling for cancer chemoprevention. Toxicol Appl Pharmacol. 2010; 244:66–76. [PubMed: 19732782]
2. Copple IM, Goldring CE, Kitteringham NR, Park BK. The keap1-nrf2 cellular defense pathway: mechanisms of regulation and role in protection against drug-induced toxicity. Handb Exp Pharmacol. 2010:233–266. [PubMed: 20020265]
3. Joshi G, Johnson JA. The Nrf2-ARE Pathway: A Valuable Therapeutic Target for the Treatment of Neurodegenerative Diseases. Recent Pat CNS Drug Discov. 2012; 7:218–229. [PubMed: 22742419]
4. Li J, Ichikawa T, Janicki JS, Cui T. Targeting the Nrf2 pathway against cardiovascular disease. Expert Opin Ther Targets. 2009; 13:785–794. [PubMed: 19530984]
5. Reuter S, Gupta SC, Chaturvedi MM, Aggarwal BB. Oxidative stress, inflammation, and cancer: how are they linked? Free Radic Biol Med. 2010; 49:1603–1616. [PubMed: 20840865]
6. Khansari N, Shakiba Y, Mahmoudi M. Chronic inflammation and oxidative stress as a major cause of age-related diseases and cancer. Recent Pat Inflamm Allergy Drug Discov. 2009; 3:73–80. [PubMed: 19149749]
7. Dinkova-Kostova AT, Holtzclaw WD, Kensler TW. The role of Keap1 in cellular protective responses. Chem Res Toxicol. 2005; 18:1779–1791. [PubMed: 16359168]
8. Zhang DD. Mechanistic studies of the Nrf2-Keap1 signaling pathway. Drug Metab Rev. 2006; 38:769–789. [PubMed: 17145701]
9. McMahon M, Thomas N, Itoh K, Yamamoto M, Hayes JD. Dimerization of substrate adaptors can facilitate cullin-mediated ubiquitylation of proteins by a “tethering” mechanism: a two-site interaction model for the Nrf2-Keap1 complex. J Biol Chem. 2006; 281:24756–24768. [PubMed: 16790436]
10. Kobayashi M, Li L, Iwamoto N, Nakajima-Takagi Y, Kaneko H, Nakayama Y, Eguchi M, Wada Y, Kumagai Y, Yamamoto M. The antioxidant defense system Keap1-Nrf2 comprises a multiple sensing mechanism for responding to a wide range of chemical compounds. Mol Cell Biol. 2009; 29:493–502. [PubMed: 19001094]
11. Yamamoto T, Suzuki T, Kobayashi A, Wakabayashi J, Maher J, Motohashi H, Yamamoto M. Physiological significance of reactive cysteine residues of Keap1 in determining Nrf2 activity. Mol Cell Biol. 2008; 28:2758–2770. [PubMed: 18268004]

12. Rachakonda G, Xiong Y, Sekhar KR, Stamer SL, Liebler DC, Freeman ML. Covalent modification at Cys151 dissociates the electrophile sensor Keap1 from the ubiquitin ligase CUL3. Chem Res Toxicol. 2008; 21:705–710. [PubMed: 18251510]
13. Eggler AL, Small E, Hannink M, Mesecar AD. Cul3-mediated Nrf2 ubiquitination and antioxidant response element (ARE) activation are dependent on the partial molar volume at position 151 of Keap1. Biochem J. 2009; 422:171–180. [PubMed: 19489739]
14. Zhang DD, Hannink M. Distinct cysteine residues in Keap1 are required for Keap1-dependent ubiquitination of Nrf2 and for stabilization of Nrf2 by chemopreventive agents and oxidative stress. Mol Cell Biol. 2003; 23:8137–8151. [PubMed: 14585973]
15. Kansanen E, Bonacci G, Schopfer FJ, Kuosmanen SM, Tong KI, Leinonen H, Woodcock SR, Yamamoto M, Carlberg C, Yla-Herttuala S, Freeman BA, Levonen AL. Electrophilic nitro-fatty acids activate NRF2 by a KEAP1 cysteine 151-independent mechanism. J Biol Chem. 2011; 286:14019–14027. [PubMed: 21357422]
16. Taguchi K, Motohashi H, Yamamoto M. Molecular mechanisms of the Keap1-Nrf2 pathway in stress response and cancer evolution. Genes Cells. 2011; 16:123–140. [PubMed: 21251164]
17. Kobayashi A, Kang MI, Watai Y, Tong KI, Shibata T, Uchida K, Yamamoto M. Oxidative and electrophilic stresses activate Nrf2 through inhibition of ubiquitination activity of Keap1. Mol Cell Biol. 2006; 26:221–229. [PubMed: 16354693]
18. Hur W, Sun Z, Jiang T, Mason DE, Peters EC, Zhang DD, Luesch H, Schultz PG, Gray NS. A small-molecule inducer of the antioxidant response element. Chem Biol. 2010; 17:537–547. [PubMed: 20534351]
19. Liu Y, Kern JT, Walker JR, Johnson JA, Schultz PG, Luesch H. A genomic screen for activators of the antioxidant response element. Proc Natl Acad Sci U S A. 2007; 104:5205–10. [PubMed: 17360324]
20. Fitzgerald V, Mensack M, Wolfe P, Thompson H. A transfer-less, multi-well liquid culture feeding system for screening small molecules that affect the longevity of Caenorhabditis elegans. Biotechniques. 2009; 47:ix–xv. [PubMed: 20041852]
21. Moy T, Conery A, Larkins-Ford J, Wu G, Mazitschek R, Casadei G, Lewis K, Carpenter A, Ausubel F. High-Throughput Screen for Novel Antimicrobials using a Whole Animal Infection Model. Acs Chemical Biology. 2009; 4:527–533. [PubMed: 19572548]
22. Dengg M, van Meel JC. Caenorhabditis elegans as model system for rapid toxicity assessment of pharmaceutical compounds. J Pharmacol Toxicol Methods. 2004; 50:209–214. [PubMed: 15519907]
23. Choe KP, Przybysz AJ, Strange K. The WD40 repeat protein WDR-23 functions with the CUL4/DDB1 ubiquitin ligase to regulate nuclear abundance and activity of SKN-1 in *Caenorhabditis elegans*. Mol Cell Biol. 2009; 29:2704–2715. [PubMed: 19273594]
24. Hasegawa K, Miwa J. Genetic and Cellular Characterization of Caenorhabditis elegans Mutants Abnormal in the Regulation of Many Phase II Enzymes. Plos One. 2010; 5:e11194. [PubMed: 20585349]
25. Choe KP, Leung CK, Miyamoto MM. Unique structure and regulation of the nematode detoxification gene regulator, SKN-1: implications to understanding and controlling drug resistance. Drug Metab Rev. 2012; 44:209–223. [PubMed: 22656429]
26. Nassar AEF, Kamel AM, Clarimont C. Improving the decision-making process in the structural modification of drug candidates: enhancing metabolic stability. Drug Discovery Today. 2004; 9:1020–1028. [PubMed: 15574318]
27. Di L, Kerns EH, Gao N, Li SQ, Huang Y, Bourassa JL, Huryn DM. Experimental design on single-time-point high-throughput microsomal stability assay. J Pharm Sci. 2004; 93:1537–1544. [PubMed: 15124211]
28. Thimmulappa RK, Mai KH, Srisuma S, Kensler TW, Yamamoto M, Biswal S. Identification of Nrf2-regulated genes induced by the chemopreventive agent sulforaphane by oligonucleotide microarray. Cancer Res. 2002; 62:5196–5203. [PubMed: 12234984]
29. Talalay P, De Long MJ, Prochaska HJ. Identification of a common chemical signal regulating the induction of enzymes that protect against chemical carcinogenesis. Proc Natl Acad Sci U S A. 1988; 85:8261–8265. [PubMed: 3141925]

30. Morales-Sanfrutos J, Lopez-Jaramillo FJ, Hernandez-Mateo F, Santoyo-Gonzalez F. Vinyl sulfone bifunctional tag reagents for single-point modification of proteins. J Org Chem. 2010; 75:4039–4047. [PubMed: 20496947]

31. Deneke SM, Fanburg BL. Regulation of cellular glutathione. Am J Physiol. 1989; 257:L163–173. [PubMed: 2572174]

32. Lee JM, Moehlenkamp JD, Hanson JM, Johnson JA. Nrf2-dependent activation of the antioxidant responsive element by tert-butylhydroquinone is independent of oxidative stress in IMR-32 human neuroblastoma cells. Biochem Biophys Res Commun. 2001; 280:286–292. [PubMed: 11162512]

33. Zago MP, Mackenzie GG, Adamo AM, Keen CL, Oteiza PI. Differential modulation of MAP kinases by zinc deficiency in IMR-32 cells: role of H_2O_2. Antioxid Redox Signal. 2005; 7:1773–1782. [PubMed: 16356139]

34. Townsend DM, Tew KD, Tapiero H. The importance of glutathione in human disease. Biomed Pharmacother. 2003; 57:145–155. [PubMed: 12818476]

35. Miao W, Hu L, Scrivens PJ, Batist G. Transcriptional regulation of NF-E2 p45-related factor (NRF2) expression by the aryl hydrocarbon receptor-xenobiotic response element signaling pathway: direct cross-talk between phase I and II drug-metabolizing enzymes. J Biol Chem. 2005; 280:20340–20348. [PubMed: 15790560]

36. Wang R, Paul VJ, Luesch H. Seaweed extracts and unsaturated fatty acid constituents from the green alga *Ulva lactuca* as activators of the cytoprotective Nrf2-ARE pathway. Free Radic Biol Med. 2013; 57:141–153. [PubMed: 23291594]

37. Lee JM, Hanson JM, Chu WA, Johnson JA. Phosphatidylinositol 3-kinase, not extracellular signal-regulated kinase, regulates activation of the antioxidant-responsive element in IMR-32 human neuroblastoma cells. J Biol Chem. 2001; 276:20011–6. [PubMed: 11274155]

38. Zipper LM, Mulcahy RT. Erk activation is required for Nrf2 nuclear localization during pyrrolidine dithiocarbamate induction of glutamate cysteine ligase modulatory gene expression in HepG2 cells. Toxicol Sci. 2003; 73:124–134. [PubMed: 12657749]

39. Rojo AI, Medina-Campos ON, Rada P, Zuniga-Toala A, Lopez-Gazcon A, Espada S, Pedraza-Chaverri J, Cuadrado A. Signaling pathways activated by the phytochemical nordihydroguaiaretic acid contribute to a Keap1-independent regulation of Nrf2 stability: Role of glycogen synthase kinase-3. Free Radic Biol Med. 2012; 52:473–487. [PubMed: 22142471]

40. Chowdhry S, Zhang Y, McMahon M, Sutherland C, Cuadrado A, Hayes JD. Nrf2 is controlled by two distinct beta-TrCP recognition motifs in its Neh6 domain, one of which can be modulated by GSK-3 activity. Oncogene. 2012 (Epub Sept 10). 10.1038/onc.2012.388

41. Zhang DD, Lo SC, Cross JV, Templeton DJ, Hannink M. Keap1 is a redox-regulated substrate adaptor protein for a Cul3-dependent ubiquitin ligase complex. Mol Cell Biol. 2004; 24:10941–10953. [PubMed: 15572695]

42. Leung CK, Deonarine A, Strange K, Choe KP. High-throughput screening and biosensing with fluorescent C. elegans strains. J Vis Exp. 2011; 51:e2745.

43. Blackwell TK, Bowerman B, Priess JR, Weintraub H. Formation of a monomeric DNA binding domain by Skn-1 bZIP and homeodomain elements. Science. 1994; 266:621–628. [PubMed: 7939715]

44. Hong F, Sekhar KR, Freeman ML, Liebler DC. Specific patterns of electrophile adduction trigger Keap1 ubiquitination and Nrf2 activation. J Biol Chem. 2005; 280:31768–31775. [PubMed: 15985429]

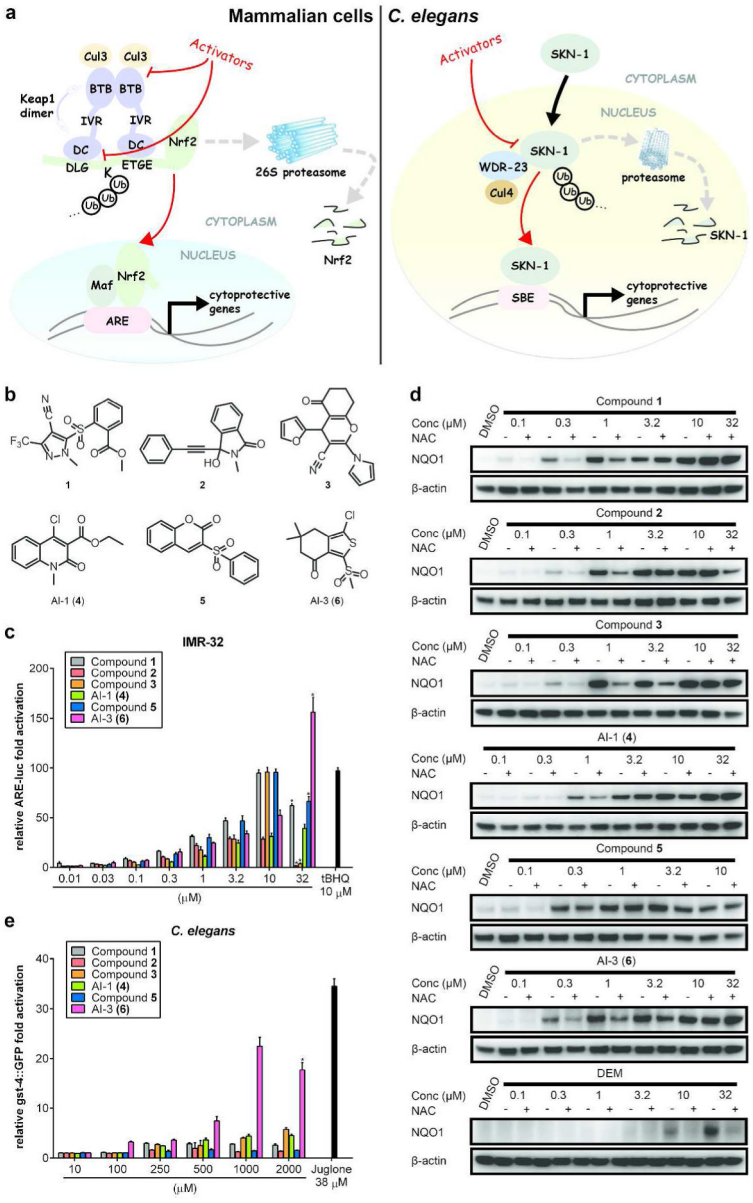

Figure 1.

Comparison of the bioactivities of prioritized Nrf2-ARE inducers *in vitro* and *in vivo*. (a) The working models of the antioxidant defense pathways in mammals and *C. elegans* (SBE, SKN-1 binding element[43]). (b) Chemical structures of the six inducers previously reported[18]. (c) Dose-dependent activation of an ARE-luciferase (ARE-luc) reporter in IMR-32 cells ($n = 3$) with 24 h of treatment. (d) 24 h after treatment, all compounds dose-dependently induced the expression of NQO1 in IMR-32 cells. At the highest active and non-toxic concentration (10 μM), the levels of induction were not reduced in the presence of an antioxidant, *N*-acetylcysteine (NAC, 1 mM), by the treatment with the same compound. (e) 24 h after treatment, AI-3 (**6**) activated a *Pgst-4* reporter transgene to much greater extent than the other five compounds in *C. elegans* ($n = 3$). Results from (c) and (e) are shown as fold activation + the standard error of the mean (SEM). Asterisk (*) designates observed toxicity.

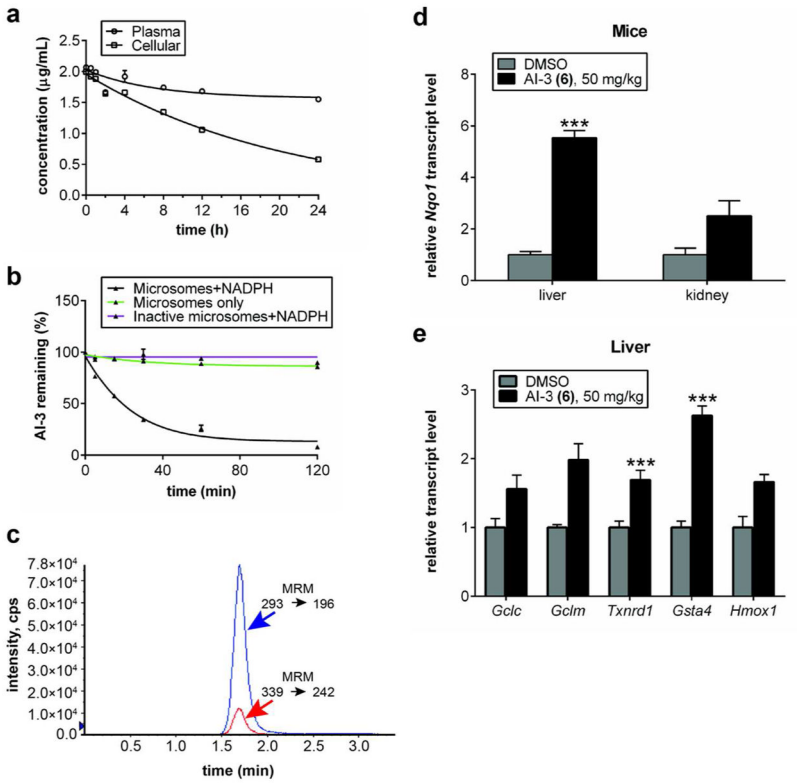

Figure 2.

Stability and rodent *in vivo* activity of AI-3. Plasma and cellular stabilities (a) and microsomal stability (b) of AI-3 ($n = 2$). (c) A representative LC-MS (MRM scan) profile of AI-3 (blue) and the bromo analog (AI-3-4) as internal standard (red). (d) AI-3 significantly upregulated the levels of *Nqo1* mRNAs in liver and kidney tissues in mice ($n = 3$) after 12 h of a single-dose i.p. treatment. (e) AI-3 induces multiple other Nrf2-ARE regulated cytoprotective genes in the liver tissues. *Gclc* (glutamate-cysteine ligase, catalytic subunit), *Gclm* (glutamate-cysteine ligase, modifier subunit), *Txnrd1*(thioredoxin reductase 1), *Gsta4* (glutathione *S*-transferase alpha-4), and *Hmox1* (heme oxygenase 1). Results are shown as fold activation + SEM. ***: $P < 0.05$.

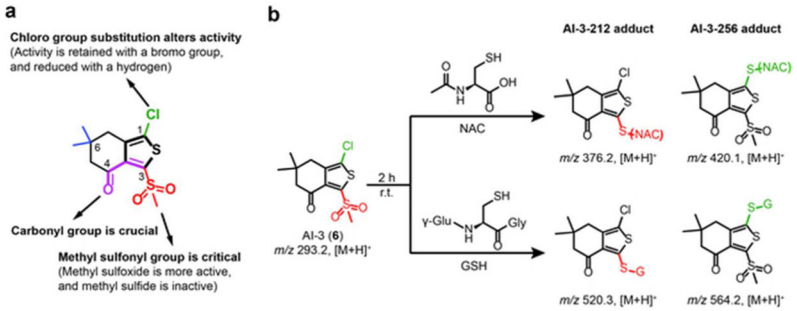

Figure 3.

The structure-activity relationships (SAR) of AI-3. (a) Summary of SAR analysis. (b) Both methyl sulfonyl and the chloro-bearing carbons are reactive towards thiols *in vitro*.

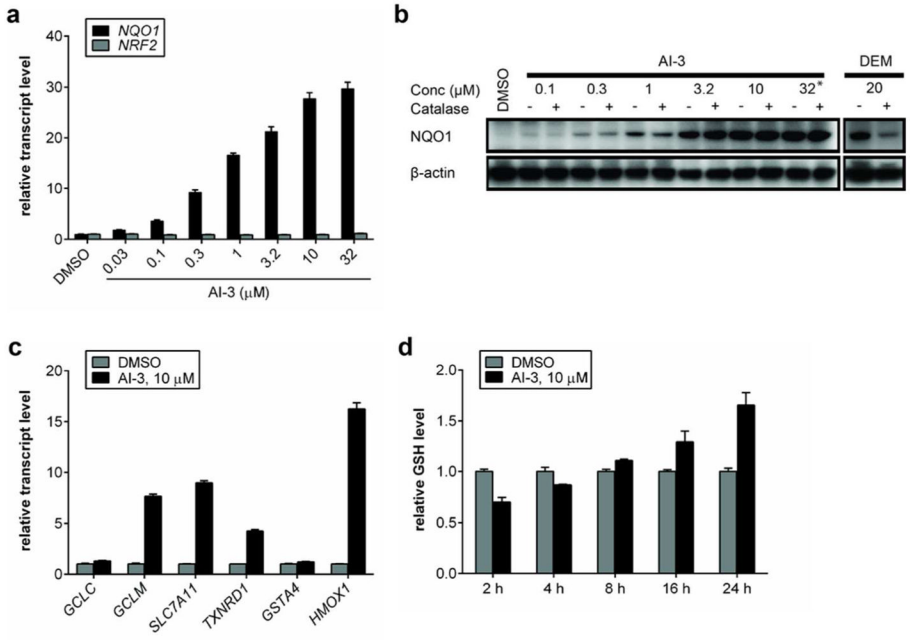

Figure 4.

AI-3 induces cytoprotective gene expression in IMR-32 cells. (a) 12 h after treatment, AI-3 induces the *NQO1* at the transcript levels ($n = 2$). (b) 24 h after treatment, AI-3 induced NQO1 protein expression starting from 0.3 μM. The presence of an antioxidant (catalase, 50 μg/ml) did not have a significant effect on AI-3's ability to induce NQO1 at all active doses tested, which is different from the result for diethyl maleate (DEM). (c) At 10 μM, AI-3 also induced other Nrf2-ARE regulated genes, *Slc7a11* (solute carrier family 7 (cationic amino acid transporter, y+ system), member 11). (d) Following a transient reduction in cellular glutathione (GSH), AI-3 induced GSH synthesis starting from 4 h up to 24 h ($n = 3$). Results from (a), (b), and (c) are shown as fold activation + SEM. Asterisk (*) designates observed toxicity.

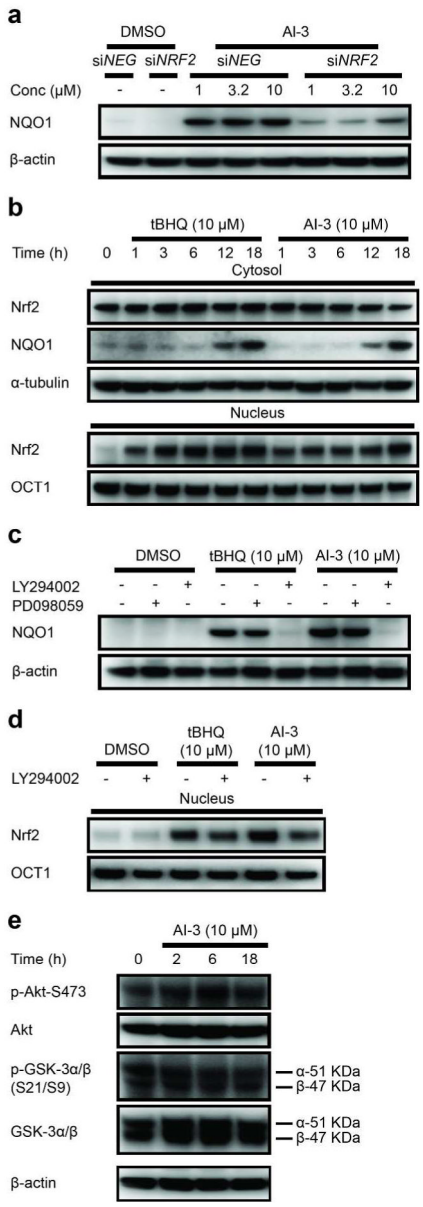

Figure 5.

Cytoprotective gene activation by AI-3 is dependent on Nrf2 and PI3K signaling pathways in IMR-32 cells. (a) 24 h of treatment with AI-3 was unable to induce NQO1 expression when endogenous *NRF2* is knocked down by small interfering RNAs (si*NRF2*). (b) AI-3 promotes the stabilization and/or nuclear translocation of Nrf2 starting from 1 h. (c) Co-treatment with LY294002 (25 μM, PI3K inhibitor), but not PD98059 (50 μM, MEK1 inhibitor), prevented AI-3-induced NQO1 expression after 24 h of treatment. (d) Co-treatment with LY294002 (25 μM, PI3K inhibitor) reduced the Nrf2 levels in the nucleus after 18 h. (e) Treatment with AI-3 did not have a profound effect on the phosphorylation status of Akt (Ser473) or GSK-3α (Ser21)/3β(Ser9).

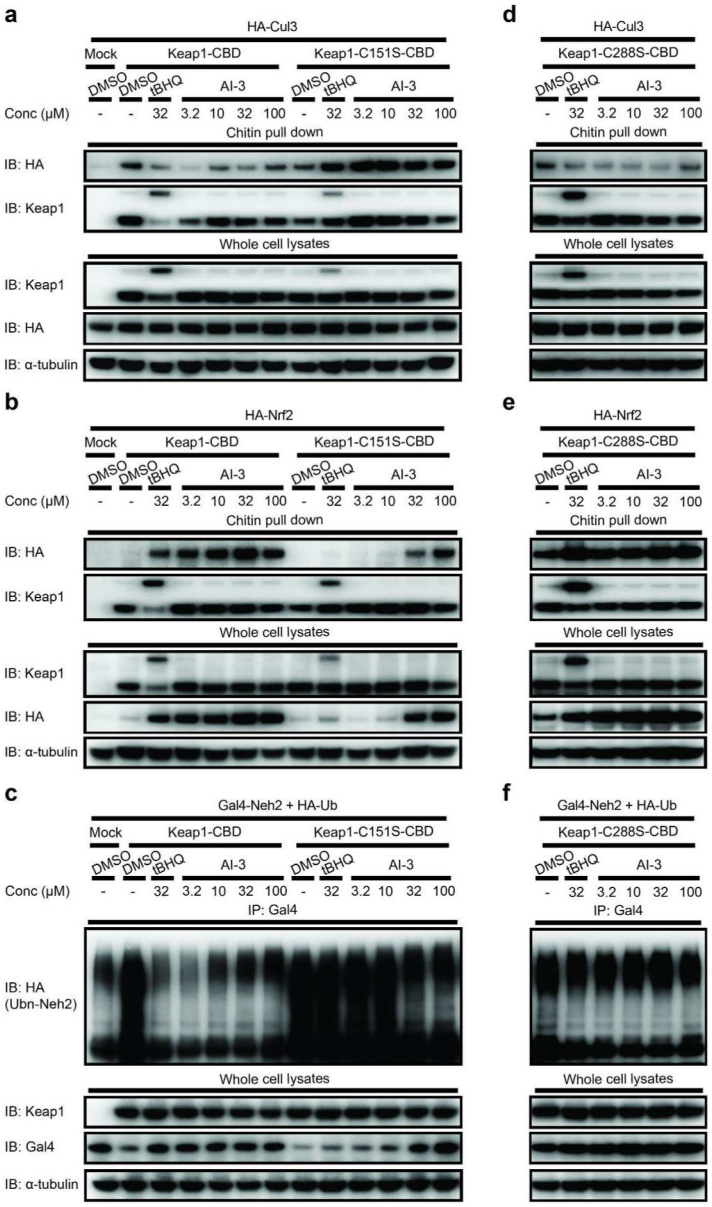

Figure 6.

AI-3 requires primarily one cysteine code (Cys151) to influence Keap1's interactions with its molecular partners. (a) 5 h of treatment with AI-3 disrupted the interactions between wild type-Keap1, but not Keap1-C151S, and Cul3. (b) 5 h of treatment with AI-3 induces the stabilization of Nrf2 in the presence of its repressor, wild type-Keap1. AI-3 can reverse the repression effect of Keap1-C151S starting from 32 μM. (c) Wild type-Keap1 facilitated Neh2 (the Keap1-binding domain of Nrf2) ubiquitination was inhibited by AI-3 after 5 h of treatment. Keap1-C151S targeted Neh2 degradation was also inhibited by AI-3 at higher doses (32 μM and 100 μM). Mock plasmid: pcDNA3-mRFP. (d) 5 h of treatment with AI-3 disrupted the interactions between Keap1-C288S and Cul3. (e) Regardless of the treatment, Nrf2 is stabilized in the presence of Keap1-C288S. (f) Regardless of the treatment, Keap1-C288S was not able to render Neh2 for ubiquitination. Note: The decreased levels of HA-Nrf2 and Gal4-Neh2 in the whole cell lysates in panels b and c were probably due to either Keap1 (DMSO treated cells) or Keap1-C151S mediated degradation of Nrf2 and Gal4-

Neh2, respectively. The higher molecular weight Keap1 band is a result of covalent reaction and Keap1 dimerization[44] observed for tBHQ but not for AI-3.

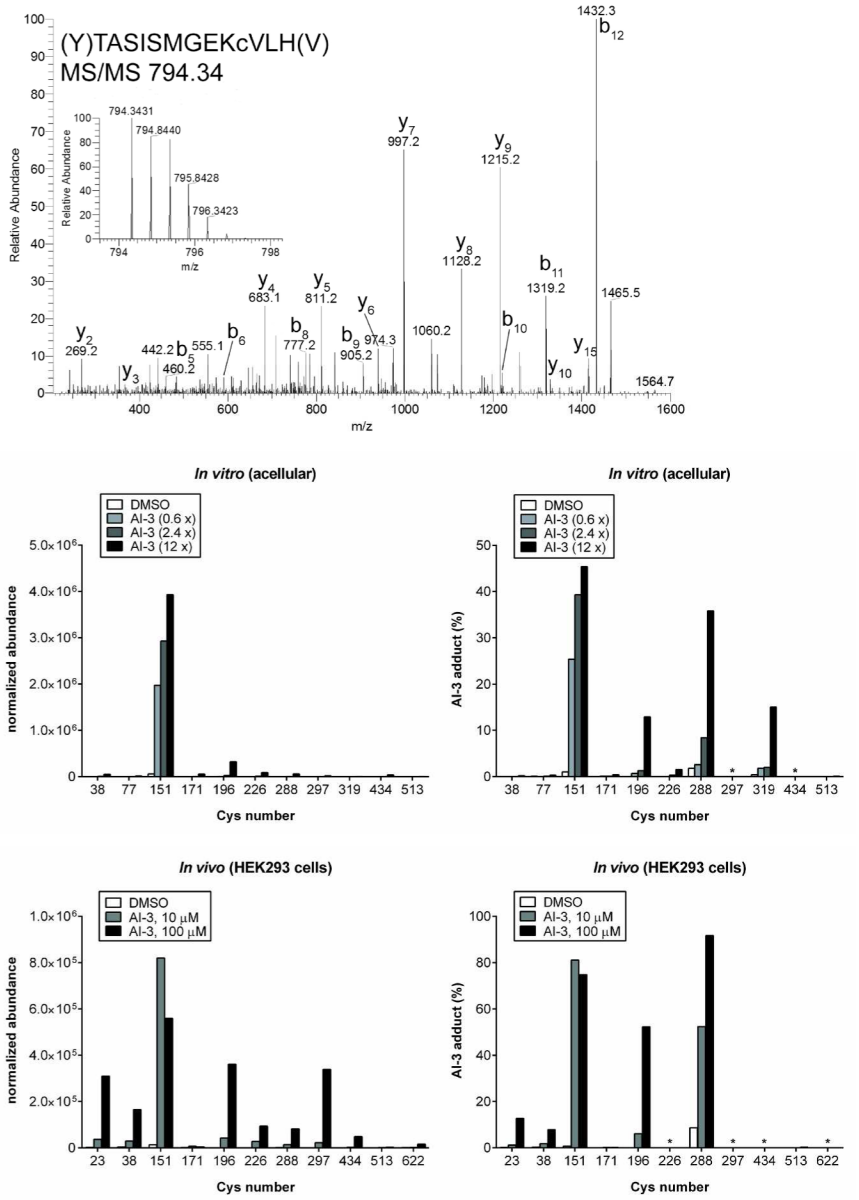

Figure 7.

AI-3 modified primarily Cys151 of Keap1 by 212 as verified by tandem LC-MS. (a) Chymotryptic peptide spectrum containing AI-3-alkylated Cys151. The inset shows the full scan accurate MS of the precursor. (b, c) *In vitro* incubation of Keap1 and AI-3. Numbers in parentheses indicate the stoichiometric ratio of AI-3 to Keap1. (d, e) Cellular incubation. HEK293 cells were transiently transfected with Keap1-CBD for 43 h then treated with AI-3 for 5 h. Keap1 was purified and digested with chymotrypsin for tandem LC-MS analysis. (b, d) Summed, normalized abundances for the peptides that contain the specified modified cysteine for the chymotrypsin digests. (c, e) Summed AI-3 (212) modified peptides divided by the sum of all forms of the peptide regardless of modification. (*) indicates that percentages for these residues could not be calculated because the corresponding unmodified peptide signal was not detected, likely due to the overall low abundance of the peptide.